Transition to one-dimensional behavior in the optical absorption of quantum-well wires

S. Glutsch and D. S. Chemla
Department of Physics, University of California, Berkeley, California 94720
and Material Sciences Division, Lawrence Berkeley National Laboratory, Berkeley, California 94720
(Received 20 December 1995)

We calculate the optical absorption of quantum-well wires for a large variety of wire widths, taking into account Coulomb interaction, unequal electron and hole effective masses, and continuum states. A transition from a two-dimensional semiconductor to a one-dimensional semiconductor is observed as the wire width is reduced. Absorption lines that are forbidden in the free-particle case appear as a result of Coulomb coupling. By comparison of different effective-mass ratios, we rigorously show that the dominant lines are related to the center-of-mass motion of excitons. The influence of a finite length and a finite thickness is studied. The one-subband approximation is found to correctly describe the extreme one-dimensional limit. A comparison with realistic dimensions, however, demonstrates the shortcoming of that approximation for quantitative predictions. [S0163-1829(96)03923-9]

I. INTRODUCTION

During the past two decades, the physics of low-dimensional semiconductors has become a vital part of present-day research. Low-dimensional structures allow the study of a variety of new mechanical, optical, and transport phenomena. In this context, one-dimensional systems have been of particular interest for the past five years. Examples are quantum-well wires,[1,2] T-shaped quantum wires,[3] V-shaped quantum wires,[4] bulk semiconductors in magnetic fields,[5] and macromolecular compounds.[6]

The optical properties of quantum wells are well understood theoretically.[7] The importance of the center-of-mass quantization for large wire widths has been demonstrated experimentally.[8] Fano resonances,[9] due to mixing of heavy-hole and light-hole states, have been observed and explained theoretically.[10] It can be shown that all excited states acquire a Fano line shape due to Coulomb interaction[11–13] and this effect can be seen on weakly allowed[14,15] and allowed[15] excitonic transitions.

The theory for quantum wires can be developed in analogy to quantum wells. However, difficulties are encountered due to the diverging behavior of the one-dimensional binding energy and the fact that the wire width is often much larger than the spatial extension of the exciton. Therefore, quantum wires have been described using discrete models,[16] effective one-dimensional potentials,[17,18] and fractal dimensions.[19] Furthermore, a number of simplifying assumptions are often made for rendering the theoretical treatment tractable, although they are not verified in real materials. For example, the electron and hole effective mass are assumed equal,[20] or the Coulomb interaction is neglected.[21]

If all intersubband transitions and the Coulomb interaction are treated correctly, the same features as for quantum wells can be expected: the center-of-mass quantization,[22] which has been previously observed experimentally;[1] and Fano resonances.[9,20] On physical grounds one can expect a smooth transition from a two-dimensional semiconductor to a one-dimensional semiconductor by narrowing a quantum-well wire. This, however, has yet to be demonstrated rigorously.

The goal of the present paper is to present optical spectra of quantum-well wires for various wire widths in order to visualize the change of dimensionality. The continuous part of the spectrum and the Coulomb interaction are taken into account fully and no assumption about electron-hole symmetry is made. This allows us to (i) separate the effects of center-of-mass and relative motion quantization, (ii) study the effects of the wire thickness and length, (iii) investigate the size dependence of the binding energy, and (iv) examine the validity of the one-subband approximation.

II. OPTICAL SPECTRUM

We use the model of a two-band semiconductor in the effective-mass approximation with masses $m_{e,h}$ for electrons and holes, respectively. The interaction with the light is mediated by a dipole matrix element μ. The static screening in the semiconductor is described by a dimensionless dielectric constant ε, which appears as a prefactor to the vacuum permittivity, $\varepsilon_0 = 8.854\,19 \times 10^{-12}$As/(Vm). Center-of-mass and relative motions of the exciton are characterized by the total mass $M = m_e + m_h$ and the reduced mass $m = m_e m_h/(m_e + m_h)$. To represent the results, we use excitonic units, the binding energy $\mathrm{Ry}^* = \frac{1}{2} m e^4/[(4\pi\varepsilon_0\varepsilon)^2\hbar^2]$, and the Bohr radius $a^* = 4\pi\varepsilon_0\varepsilon\hbar^2/(me^2)$ of the three-dimensional exciton.

We assume that the constants m_e, m_h, ε, and $\hbar\epsilon$ are known from experiments or from tables. Then, the relative mass m and the background dielectric constant determine the excitonic units Ry* and a^*. The remaining input parameters of the calculation are the effective-mass ratio m_h/m_e and the homogeneous broadening $\hbar\epsilon$ in units of Ry*. For gallium arsenide we have approximately $\mathrm{Ry}^* = 4.7$ meV, $a^* = 120$ Å, and $m_h/m_e = 7$. The homogeneous broadening depends on the sample quality and on the temperature. We assume a value of $\hbar\epsilon = 0.2$ Ry* throughout the paper.

A. Transition from a quantum well to a quantum-well wire

We consider that a quantum wire is obtained from a quantum well whose thickness is much smaller than the wire width b, so that there is almost ideal two-dimensional confinement in the z direction. We assume infinitely high barriers for the quantization in the lateral (y) direction, and free motion in the wire (x) direction. The one-dimensional optical susceptibility is then given by

$$\chi^{(1D)}(\omega)=\frac{|\mu|^2}{\varepsilon_0}\int_0^b dy\int_0^b dy'\sum_\lambda \frac{\Phi_\lambda(0,y,y)\Phi_\lambda^*(0,y',y')}{E_\lambda-\hbar(\omega+i\epsilon)}, \tag{1}$$

where

$$\left[-\frac{\hbar^2}{2m}\frac{\partial^2}{\partial x^2}-\frac{\hbar^2}{2m_e}\frac{\partial^2}{\partial y_e^2}-\frac{\hbar^2}{2m_h}\frac{\partial^2}{\partial y_h^2}-\frac{\hbar^2\pi^2}{2mb^2}-\frac{e^2}{4\pi\varepsilon_0\varepsilon\sqrt{x^2+(y_e-y_h)^2}}\right]\Phi_\lambda(x,y_e,y_h)=E_\lambda\Phi_\lambda(x,y_e,y_h), \tag{2}$$

$$x\in(-\infty,+\infty);\quad y_e,y_h\in[0,b].$$

Due to the confinement, the eigenfunctions $\Phi_\lambda(x,y_e,y_h)$ vanish for $y_e\in\{0,b\}$ or $y_h\in\{0,b\}$. The energy $\hbar^2\pi^2/(2mb^2)$ of the first subband is subtracted from the Hamiltonian, so that the continuum always starts at $\hbar\omega=0$. This assists us when we compare spectra for different wire widths. The above equations have been solved numerically in real space with a grid spacing of $0.08\ldots0.16a^*$.[23]

In Fig. 1 the optical absorption, $\mathrm{Im}\chi^{(1D)}$, of a quantum-well wire is plotted versus the excitation energy $\hbar\omega$ for $m_e=m_h$ and $b=1\ldots16a^*$. The height of the spectra is normalized. For $b=16a^*$, the spectrum is very similar to that of a quantum well: the binding energy is about 4 Ry*, which is the value for the two-dimensional exciton, and the continuum absorption is nearly constant in the displayed frequency range. The ratio of the absorption maximum and the onset of the continuum absorption is found to be 21.54, which is close to the ideal two-dimensional value $(16/\pi)(\hbar\epsilon/\ \mathrm{Ry}^*)^{-1}=25.46,\ldots$. The loss in the excitonic oscillator strength is due to the center-of-mass quantization, which manifests itself as a small modulation of the spectrum between the ground-state exciton and the continuum, and in the continuum. The distance between the maxima and minima increases when the wire width is reduced to $b=8a^*$. The spectrum for $b=4a^*$ shows that there are two types of peaks involved with, alternatively, a large and a small linewidth. For $b=2a^*$ we observe an enhancement of the binding energy. The transitions at negative energies $\hbar\omega<0$ are discrete with a Lorentzian line shape, whereas for $\hbar\omega>0$ Fano resonances[9] are formed due to the coupling of discrete and continuous states belonging to different subbands.[20] Finally, for $b=1a^*$ the continuum absorption is constant, as it was the case for large wire widths. In contrast to a quantum well, however, the binding energy is enhanced and the ratio between the absorption of the continuum edge and the exciton is smaller, as it is a characteristic feature for transitions to lower dimensions.[19]

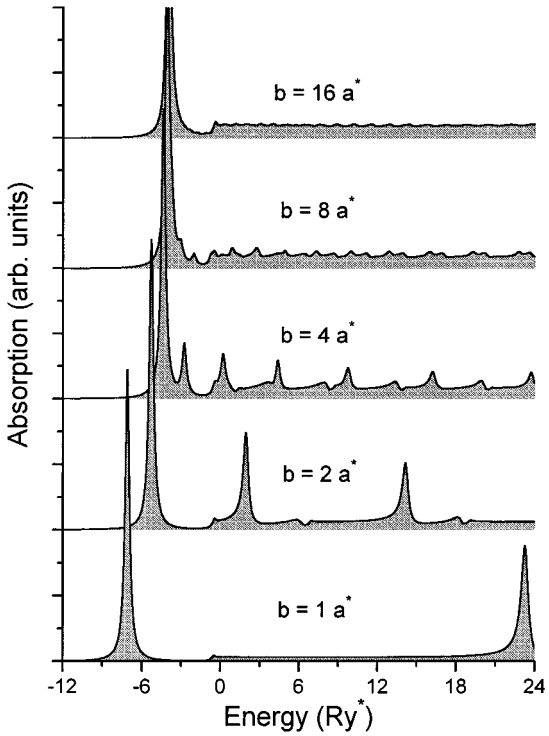

FIG. 1. Optical absorption of quantum-well wires vs energy $\hbar\omega$ for $d=0$, different wire width $b=16a^*$, $8a^*$, $4a^*$, $2a^*$, and $1a^*$, and $m_h=m_e$. The heights of the lowest transitions are normalized.

B. Influence of unequal masses for electron and hole

To explore the effects of unequal effective masses, we now consider $m_h/m_e=7$, which corresponds approximately to GaAs. No significant changes are expected in the quantum-well limit, $b\to\infty$, and in the extreme one-dimensional limit, $b\to0$, since in both cases the optical properties are governed by the relative motion only. The results for intermediate wire widths are shown in Fig. 2. Surprisingly, for $b=1a^*$ one sees an additional peak that can be attributed to the $(n_e,n_h)=(1,3)$ transition. Since the barriers are infinitely high, this transition is forbidden in the single-particle picture. The origin of this transition can be explained in the following way: all subbands with $(n_e-n_h)\ \mathrm{mod}2=0$ and $(n_e-n_h)\ \mathrm{mod}2=1$ are mutually coupled by the Coulomb interaction. Since the first system contains the allowed transitions $(n_e=n_h)$, the Coulomb coupling results in a finite transition probability for all transitions with $(n_e-n_h)\ \mathrm{mod}2=0$. This, however, does not result in discrete lines but rather in Fano resonances (see inset) because of the degeneracy with continuum states. The oscillator strength of those weakly allowed transitions decreases for narrower wires since the intersubband coupling decreases. It is worth mentioning that this effect also takes place in quantum wells. Therefore, weakly allowed transitions are not necessarily the result of wave functions' leakage through the barriers, as commonly believed.

The assignment of the absorption peaks is particularly interesting. In the limit $b\to0$, the separation of subbands even-

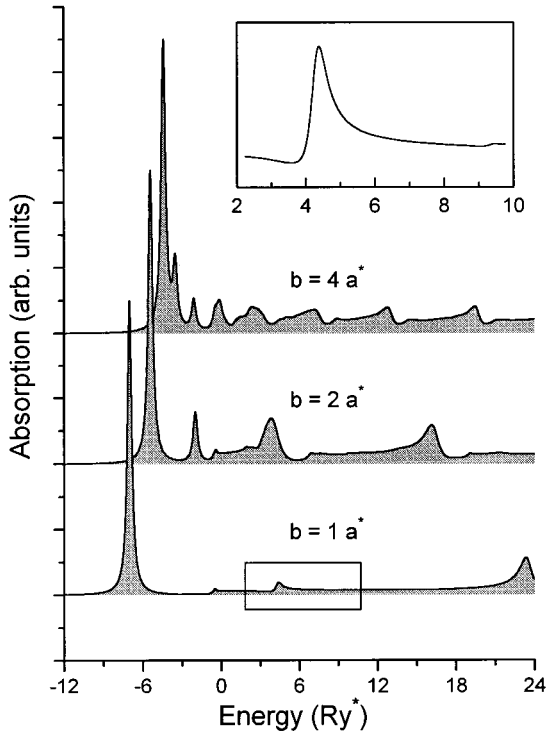

FIG. 2. Optical absorption of quantum-well wires vs energy $\hbar\omega$ for $d=0$, different wire width $b=4a^*$, $2a^*$, and $1a^*$, and $m_h=7m_e$. The heights of the lowest transitions are normalized. Inset: Closeup of the dashed box in the spectrum for $b=1a^*$.

tually exceeds the exciton binding energy, and absorption lines can be classified by the subband pair and an additional quantum number of the even-parity one-dimensional exciton. In contrast to quantum wells, quantum wires are usually far from this limit because (i) the intersubband coupling of the one-dimensional Coulomb potential is much stronger than in two dimensions, and (ii) for technical reasons the wire widths cannot be made arbitrarily small. Therefore, realistic quantum-well wires often have an intermediate thickness. In this case, we expect two types of transitions: (a) the spatially small excitons keep their internal structure but perform a center-of-mass motion between the barriers.[1,22] The spectral positions of the corresponding resonances are roughly given by $E_N=\hbar^2(2N-1)^2\pi^2/(2Md^2)-4$ Ry*, $N=1,2,3,\ldots$. (b) Even if the wire width is much larger than the excitonic Bohr radius, there is always an infinite number of excitons with a spatial extent larger than the wire with. The relative motion of those excitons is subject to size quantization and their energies will accumulate at the subband edges, $E_n=\hbar^2n^2\pi^2/(2md^2)$, $n=1,2,3,\ldots$.

The nature of the transitions can be studied by comparison of the spectra for $m_e=m_h$ (Fig. 1) and $m_e\neq m_h$ (Fig. 2) for a fixed wire width, e.g., $b=4a^*$. The free-particle absorption is identical in both cases since optical density of states is independent of the effective-mass ratio and the Rydberg units were defined in terms of the reduced mass. For $m_h/m_e=1$, the spectrum has a very regular structure and is characterized by a sequence of consecutive small and large peaks. For $m_h/m_e=7$, the small peaks stay almost at their positions, but the large ones are shifted to lower energies. We can thus conclude that the small peaks correspond to exciton size quantization, and that they appear just below the subband edges that depend on the relative mass. The large and narrow peaks originate from the center-of-mass quantization. Their energies scale according to the total mass. In the case presented here, the separation between the large peaks and the lowest transition decreases by a factor of about $\frac{16}{7}$; i.e., the change of the total mass as the mass ratio is changed from $m_h/m_e=1$ to $m_h/m_e=7$. The lines resulting from the center-of-mass motion are narrower because those excitons have a small spatial extension resulting in a weaker coupling to the continuum. It is important to note that the regular appearance of the spectrum for $m_h=m_e$ is purely accidental; for in this particular case it holds that $\hbar^2(2N-1)^2\pi^2/(2Md^2)=\hbar^2(N-\frac{1}{2})^2\pi^2/(2md^2)$.

C. Influence of a finite thickness and finite length

Quantum-well wires are often treated as if they were based on an ideal two-dimensional semiconductor, and their length was infinite. Intuitively, it is plausible that those assumptions are justified if the thickness of the underlying quantum well is much smaller than the Bohr radius of the exciton, and the length is much larger than the Bohr radius. However, it is important to have some quantitative estimate of what can be considered as ''much smaller'' and ''much larger.''

First, we consider a quantum-well wire of the size: length$\times$width$\times$thickness$=\infty\times b\times d$. The optical susceptibility is given by

$$\chi^{(1D)}(\omega)=\frac{|\mu|^2}{\varepsilon_0}\int_0^b dy\int_0^b dy'\int_0^d dz\int_0^d dz'\sum_\lambda \frac{\Phi_\lambda(0,y,y,z,z)\Phi_\lambda^*(0,y',y',z',z')}{E_\lambda-\hbar(\omega+i\epsilon)} \tag{3}$$

and

$$\left[-\frac{\hbar^2}{2m}\frac{\partial^2}{\partial x^2}-\frac{\hbar^2}{2m_e}\frac{\partial^2}{\partial y_e^2}-\frac{\hbar^2}{2m_h}\frac{\partial^2}{\partial y_h^2}-\frac{\hbar^2}{2m_e}\frac{\partial^2}{\partial z_e^2}-\frac{\hbar^2}{2m_h}\frac{\partial^2}{\partial z_h^2}-\frac{\hbar^2\pi^2}{2mb^2}-\frac{\hbar^2\pi^2}{2md^2}\right.$$
$$\left.-\frac{e^2}{4\pi\varepsilon_0\varepsilon\sqrt{x^2+(y_e-y_h)^2+(z_e-z_h)^2}}\right]\Phi_\lambda(x,y_e,y_h,z_e,z_h)=E_\lambda\Phi_\lambda(x,y_e,y_h,z_e,z_h), \tag{4}$$

$$x\in(-\infty,+\infty);\quad y_e,y_h\in[0,b];\quad z_e,z_h\in[0,d].$$

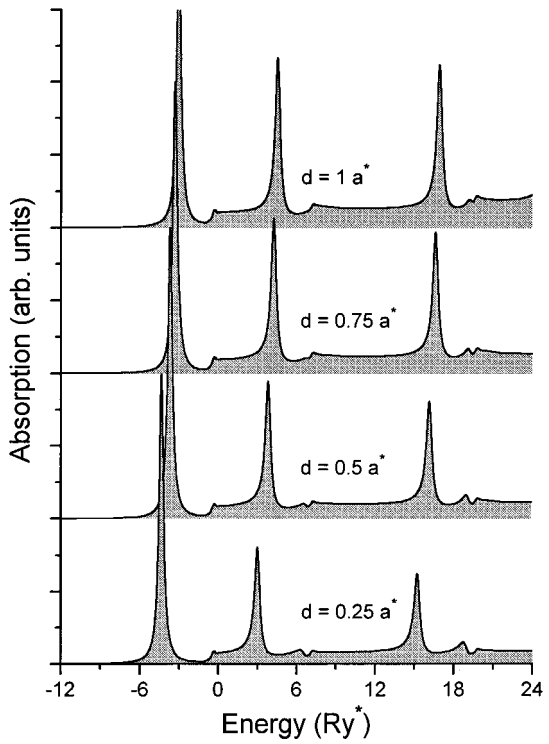

FIG. 3. Optical absorption of a quantum-well wire vs energy $\hbar\omega$, for $m_e=m_h$, a wire width $b=2a^*$, and different wire thicknesses $d=0.25a^*$, $0.5a^*$, $0.75a^*$, and $1a^*$. The heights of the lowest transitions are normalized.

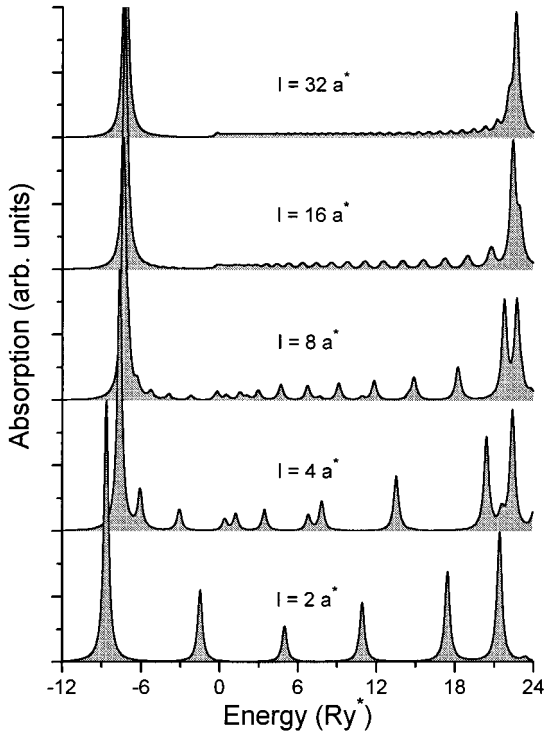

FIG. 4. Optical absorption of a quantum-well wire vs energy $\hbar\omega$, for $d=0$, $b=1a^*$, and a finite length $l=2a^*$, $4a^*$, $8a^*$, 16 a^*, and $32a^*$. The heights of the lowest transitions are normalized.

Numerical results are shown in Fig. 3 for $m_e=m_h$, a constant width $b=2a^*$, and different values of the thickness $d=1a^*$, $0.75a^*$, $0.5a^*$, and $0.25a^*$. As the thickness is reduced, the binding energy gradually increases, and the oscillator strengths of the excited main peaks ($N>1$) decrease, compared to the ground state ($N=1$). The side peaks are hardly visible for large thicknesses, but become more pronounced if d is reduced. A comparison with Fig. 1 shows that the assumption of a vanishing thickness is justified if $d\leqslant 0.25a^*$. This is about the well thickness in the experiment by Brunner *et al.*[2]

The effect of the length on the exciton binding energy in molecular chains has been studied by Fujiki.[6] In our theoretical approach, we assume a quantum-well wire of the size $l\times b\times 0$. The optical susceptibility is obtained from

$$\chi^{(1D)}(\omega)=\frac{|\mu|^2}{\varepsilon_0}\frac{1}{l}\int_0^l dx\int_0^l dx'\int_0^b dy\int_0^b dy'\sum_\lambda \frac{\Phi_\lambda(x,x,y,y)\Phi_\lambda^*(x',x',y',y')}{E_\lambda-\hbar(\omega+i\epsilon)}, \tag{5}$$

where

$$\left[-\frac{\hbar^2}{2m^e}\frac{\partial^2}{\partial x_e^2}-\frac{\hbar^2}{2m^h}\frac{\partial^2}{\partial x_h^2}-\frac{\hbar^2}{2m_e}\frac{\partial^2}{\partial y_e^2}-\frac{\hbar^2}{2m_h}\frac{\partial^2}{\partial y_h^2}-\frac{\hbar^2\pi^2}{2ml^2}-\frac{\hbar^2\pi^2}{2mb^2}-\frac{e^2}{4\pi\varepsilon_0\varepsilon\sqrt{(x_e-x_h)^2+(y_e-y_h)^2}}\right]$$
$$\times\Phi_\lambda(x_e,x_h,y_e,y_h)=E_\lambda\Phi_\lambda(x_e,x_h,y_e,y_h),\quad x_e,x_h\in[0,l];\quad y_e,y_h\in[0,b]. \tag{6}$$

Optical spectra of quantum-well wires with a fixed width $b=1$, and different lengths $l=32a^*$, $16a^*$,$8a^*$,$4a^*$, and $2a^*$ are shown in Fig. 4. The spectrum for $l=32a^*$ resembles that of an infinitely long wire (cf. Fig. 1). A small modulation shows the influence of the center-of-mass motion along the wire direction. As the length is reduced, the distance of consecutive maxima and minima increases. Eventually, for $b\leqslant 4a^*$, clear and distinct Lorentzian resonances are observed and a quantum dot, i.e., a zero-dimensional structure, is formed. A comparison with GaAs parameters shows that, in most situations, the finite length of the wire can be disregarded.

III. BINDING ENERGY

Most of the published calculations assume that only the lowest subband contributes to the optical spectrum,[18] and it

is important to check the validity of this approximation. In this section, we examine the influence of this ''one-subband approximation'' on the binding energy.

The ground state of a quantum-mechanical system, characterized by the Hamiltonian $\hat{H}$, is defined as $E_{\text{g.s.}} = \inf[\langle\Phi|\hat{H}|\Phi\rangle/\langle\Phi|\Phi\rangle]$. In the presence of Coulomb interaction, the ground-state energy $E_{\text{g.s.}}$ is lower than its value $E^{(0)}_{\text{g.s.}}$ in the absence of Coulomb interaction. The difference $E_B = E^{(0)}_{\text{g.s.}} - E_{\text{g.s.}}$ is called the exciton binding energy. Since $\hat{H}$ was chosen such that $E^{(0)}_{\text{g.s.}} = 0$, it holds that $E_B = -E_{\text{g.s.}}$.

Let $\vec{\xi}$ and $\vec{\eta}$ denote the coordinates in the direction of free motion and confinement, respectively. The one-subband approximation is characterized by a trial function $\Phi'(\vec{\xi}, \vec{\eta}_e, \vec{\eta}_h) = \varphi'(\vec{\xi})\varphi^{(0)}_{e1}(\vec{\eta}_e)\varphi^{(0)}_{h1}(\vec{\eta}_h)$, where $\varphi^{(0)}_{e,h1}$ are the ground-state eigenfunctions of the individual motion of electron and hole in the confinement directions. This is done with the understanding that, lowering the size in the confinement direction, the distance to the higher subband increases, and their influence becomes less important. The remaining eigenvalue problem for φ' leads to a binding energy $E'_B \leqslant E_B$.

A. Quantum well and quantum dot

Based on the fact that the two-dimensional Coulomb potential has a finite binding energy, it can be shown easily that the binding energy E_B is smaller than the two-dimensional value 4 Ry* and that the value E'_B from the one-subband approximation approaches 4 Ry* as the well thickness d is reduced. Since $E'_B \leqslant E_B$, it follows that both functions are asymptotically equal for $d \to 0$.

The behavior is different for zero-dimensional structures. As an example, we consider a flat, square quantum dot.[24] It is described by Eq. (6) with $l = b$, where b is the length of the side. Since in the absence of Coulomb interaction the ground state is isolated and nondegenerate, the ground-state energy, including Coulomb interaction, can be expressed by a perturbation series:

$$E_{\text{g.s.}} = -V_{1111\,1111} - \sum_{p=1}^{\infty}\sum_{q=1}^{\infty}\sum_{r=1}^{\infty}\sum_{s=1}^{\infty}\frac{|V_{1111\,p'q'r's'}|^2}{E^{(0)}_{p'q'r's'} - E^{(0)}_{1111}} + O\left(\frac{1}{b}\right),$$

where

$$E^{(0)}_{pqrs} = \frac{(p-1)^2\pi^2}{2m_e b^2} + \frac{(q-1)^2\pi^2}{2m_h b^2} + \frac{(r-1)^2\pi^2}{2m_e b^2} + \frac{(s-1)^2\pi^2}{2m_h b^2},$$

$$\Phi^{(0)}_{pqrs}(x_e, x_h, y_e, y_h) = \sqrt{2/b}\sin\left(\frac{p\pi x_e}{b}\right)\sqrt{2/b}\sin\left(\frac{q\pi x_h}{b}\right) \times \sqrt{2/b}\sin\left(\frac{r\pi y_e}{b}\right)\sqrt{2/b}\sin\left(\frac{s\pi y_h}{b}\right),$$

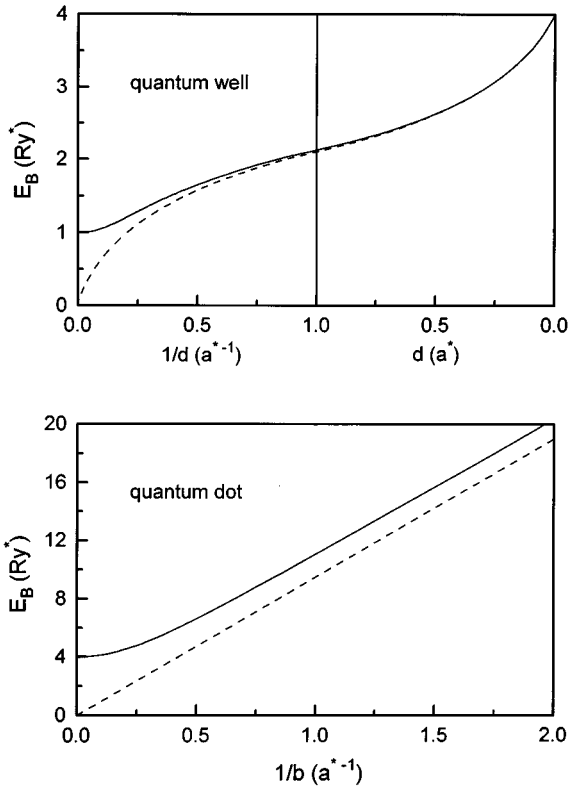

FIG. 5. Comparison of exact binding energies (solid line) with the result of the one-subband approximation (dashed line) for a quantum well (top) and a flat, square quantum dot (bottom). The parameter is the thickness d for quantum wells and the length of the side b for quantum dots.

$$V_{pqrsp'q'r's'} = \int_0^b dx_e \int_0^b dx_h \int_0^b dy_e \int_0^b dy_h \Phi^{(0)*}_{pqrs}(x_e, x_h, y_e, y_h) \times \frac{e^2}{4\pi\varepsilon_0\varepsilon\sqrt{(x_e - x_h)^2 + (y_e - y_h)^2}} \times \Phi^{(0)}_{p'q'r's'}(x_e, x_h, y_e, y_h).$$

From $V_{pqrsp'q'r's'} \propto 1/b$ it follows that the second contribution to $E_{\text{g.s.}}$ is independent of b. Hence, the asymptotic behavior of the binding energy is $E_B \sim E'_B + c$, where c is a positive constant. This result is rather general and follows from the discrete nature of the spectrum and from the scaling behavior of the zeroth-order energies and the Coulomb matrix elements with the characteristic length of the quantum dot.[25,26]

Figure 5 shows the binding energy E_B (solid line) and the result of the one-subband approximation (dashed line) for a quantum well with thickness d and a flat, square quantum dot with width b. As the best case, we chose $m_e = m_h$, which underestimates the binding energy. For quantum wells (top) the binding energy starts at the three-dimensional Ry* for infinite thickness and approaches the ideal two-dimensional value 4 Ry* as the thickness d approaches zero. The one-subband approximation leads to accurate results for $d \leqslant 1a^*$. For the quantum dot (bottom), the approximate

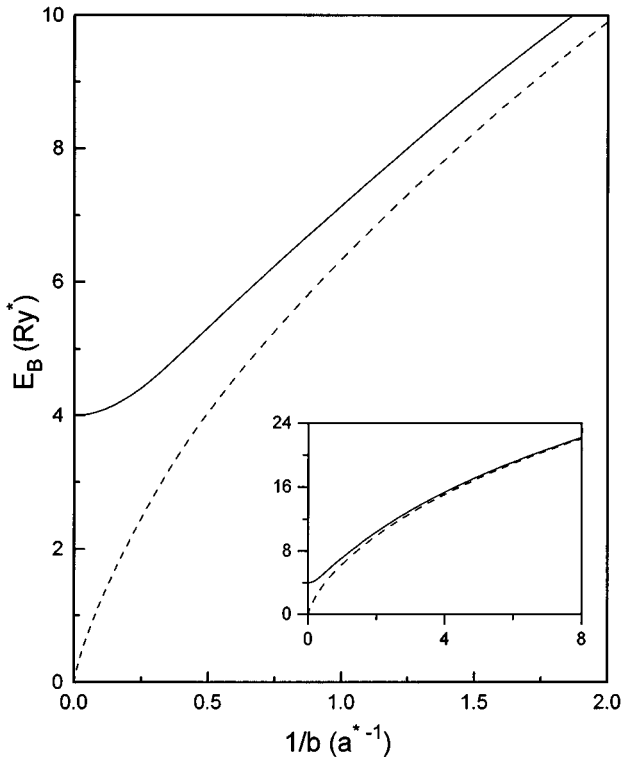

FIG. 6. Comparison of exact binding energies (solid line) with those resulting from the one-subband approximation (dashed line) vs the inverse wire width $1/b$. Inset: The same function for a larger range of $1/b$.

binding energy $E_B' = V_{1111\,1111} = \alpha e^2/(4\hbar\varepsilon_0\varepsilon b)$; $\alpha = 4.7588\ldots$ never approaches the true binding energy but differs from E_B by a constant, as b goes to zero.

B. Quantum-well wires

Apparently, the arguments used in the last subsection cannot be applied to one-dimensional structures; neither is the binding energy of the one-dimensional Coulomb potential finite, nor is the density of states completely discrete. Therefore, we calculate numerically the binding energy from Eq. (2), and the one-subband approximation corresponds to the ansatz

$$\Phi'(x,y_e,y_h) = \varphi'(x)\sqrt{2/b}\sin\left(\frac{\pi y_e}{b}\right)\sqrt{2/b}\sin\left(\frac{\pi y_h}{b}\right).$$

In Fig. 5, the dependence of the binding energy of a quantum-well wire (solid line) is compared with the one-subband approximation (dashed line). Equal masses for electron and hole are assumed. The binding energy starts at the two-dimensional value 4 Ry* and goes to infinity as the wire width b approaches zero. The increase is sublinear with $1/b$, and eventually the approximate result converges towards the exact one (inset). However, the convergence is much worse than for quantum wells. The end of the abscissa corresponds to 6 nm for GaAs, whereas the lowest experimental values obtained in T-shaped wires are between 7 and 12.5 nm.[3] This demonstrates that the one-subband approximation cannot be applied to realistic structures.

IV. SUMMARY

In summary, we have demonstrated the dimensionality transition in quantum-well wires from a two- to a one-dimensional semiconductor. Due to the Coulomb coupling of different subband pairs, forbidden transitions can become optically active. The structure of the absorption spectrum of quantum well wires, which can be explained in terms of center-of-mass and size quantization, varies considerably with the mass ratio between electrons and holes.

The model of a perfectly flat quantum wire was found to accurately describe the physical properties for a wire width lower than, or equal to, $0.25a^*$. A transition to a zero-dimensional structure can be observed if the length of the wire is reduced.

In contrast to quantum dots, the one-subband approximation yields a binding energy that slowly converges towards the exact one as the wire width is reduced. However, the convergence is much slower than for quantum wells, and is of no practical use for realistic wire widths.

ACKNOWLEDGMENTS

The authors wish to thank S. Bar-Ad, F. Bechstedt, H. Eschrig, G. Jungk, P. Kner, K. Leo, S.G. Louie, B. Pfrommer, P.E. Simmonds, M.S. Skolnick, D.S. Tekorius, and R. Zimmermann for helpful discussions. This work was supported by the Director, Office of Energy Research, Office of Basic Energy Sciences, Division of Material Sciences of the U.S. Department of Energy, under Contract No. DE-AC03-76SF00098. The financial support from the Deutsche Forschungsgemeinschaft (S.G.) is gratefully acknowledged.

[1] H. Lage, D. Heitmann, R. Cingolani, P. Grambow, and K. Ploog, Phys. Rev. B **44**, 6550 (1991).
[2] K. Brunner, G. Abstreiter, M. Walther, G. Böhm, and G. Tränkle, Surf. Sci. **267**, 218 (1992).
[3] W. Wegscheider, L.N. Pfeiffer, M.M. Dignam, K. West, S.L. McCall, and R. Hull, Phys. Rev. Lett. **71**, 4071 (1993); T. Someya, H. Akiyama, and H. Sakaki, *ibid.* **74**, 3664 (1995).
[4] R. Rinaldi *et al.*, Phys. Rev. Lett. **73**, 2899 (1994).
[5] W. Becker, B. Gerlach, T. Hornung, and R.G. Ulbrich, in *Proceedings of the 18th International Conference on the Physics of Semiconductors, Stockholm, Sweden, 1986*, edited by O. Engström (World Scientific, Singapore, 1987); S. Glutsch, U. Siegner, M.-A. Mycek, and D.S. Chemla, Phys. Rev. B **50**, 17 009 (1994).
[6] M. Fujiki, Appl. Phys. Lett. **65**, 3251 (1994).
[7] For a comprehensive review, see R. Cingolani and R. Rinaldi, Rivista del Nuovo Cimento **16**, 1 (1993); R. Winkler, Phys. Rev. B **51**, 14 395 (1995).
[8] H. Tuffigo *et al.*, J. Cryst. Growth **101**, 778 (1990).
[9] U. Fano, Phys. Rev. **124**, 1866 (1961).
[10] D.A. Broido and S.-R.E. Yang, Phys. Rev. B **42**, 11 051 (1990).
[11] H. Chu and Y.-C. Chang, Phys. Rev. B **39**, 10 861 (1989).

[12] J.A. Brum and D. Oberli, J. Phys. (France) IV Colloq. **3**, C5-191 (1993).
[13] A.R.K. Willcox and D.M. Whittaker, Superlattices Microstruct. **16**, 59 (1994).
[14] D.Y. Oberli, G. Böhm, G. Weimann, and J.A. Brum, Phys. Rev. B **49**, 5757 (1994).
[15] P.E. Simmonds *et al.*, Phys. Rev. B **50**, 11 251 (1994).
[16] K. Ishida, H. Aoki, and T. Chikyu, Phys. Rev. B **47**, 7594 (1993); G.W. Bryant, *ibid.* **49**, 16 129 (1994); Th. Östreich, K. Schönhammer, and L.J. Sham, Phys. Rev. Lett. **74**, 4698 (1995).
[17] T. Ogawa and T. Takagahara, Phys. Rev. B **44**, 8138 (1991).
[18] L. Bányai, I. Galbraith, C. Ell, and H. Haug, Phys. Rev. B **36**, 6099 (1987); B.A. Nguyen and H. Haug, *ibid.* **46**, 9569 (1992); S. Benner and H. Haug, *ibid.* **47**, 15 750 (1993); A.L. Ivanov and H. Haug, Phys. Rev. Lett. **71**, 3182 (1993).
[19] P. Lefebvre, P. Christol, and H. Mathieu, Phys. Rev. B **48**, 17 308 (1993).
[20] S. Glutsch, D.S. Chemla, and F. Bechstedt, Phys. Rev. B **51**, 16 885 (1995).
[21] U. Bockelmann and G. Bastard, Phys. Rev. B **45**, 1700 (1992); C.R. McIntyre and L.J. Sham, *ibid.* **45**, 9443 (1992).
[22] S. Glutsch and F. Bechstedt, Phys. Rev. B **47**, 4315 (1993); **47**, 6385 (1993); A. D'Andrea and L. Pilozzi, J. Phys. (France) IV **3**, C5-385 (1993).
[23] S. Glutsch (unpublished).
[24] K. Brunner *et al.*, Phys. Rev. Lett. **69**, 3216 (1992).
[25] B. Adolph, S. Glutsch, and F. Bechstedt, Phys. Rev. B **48**, 15 077 (1993).
[26] A.H. MacDonald and S. Ritchie, Phys. Rev. B **33**, 8336 (1986).